

## Dynamic blood brain barrier regulation in mild head trauma

Eoin O’Keeffe<sup>1§</sup>, Eoin Kelly<sup>2§</sup>, Yuzhe Liu<sup>3</sup>, Chiara Giordano<sup>3</sup>, Eugene Wallace<sup>2</sup>, Mark Hynes<sup>4</sup>, Stephen Tiernan<sup>5</sup>, Aidan Meagher<sup>5</sup>, Chris Greene<sup>1</sup>, Stephanie Hughes<sup>6</sup>, Tom Burke<sup>7</sup>, John Kealy<sup>1</sup>, Niamh Doyle<sup>6</sup>, Alison Hay<sup>2</sup>, Michael Farrell<sup>8</sup>, Gerald A. Grant<sup>9</sup>, Alon Friedman<sup>10,11</sup>, Ronel Veksler<sup>10</sup>, Michael G. Molloy<sup>12</sup>, James F. Meaney<sup>13</sup>, Niall Pender<sup>6</sup>, David Camarillo<sup>3#</sup>, Colin P. Doherty<sup>2,7\*\*</sup>, and Matthew Campbell<sup>1\*\*</sup>.

<sup>1</sup>Smurfit Institute of Genetics, Trinity College Dublin, Dublin 2, Ireland.

<sup>2</sup>Department of Neurology, Health Care Centre, Hospital 5, St James's Hospital, Dublin 8, Ireland.

<sup>3</sup>Department of Mechanical Engineering, Stanford University, Stanford, CA 94305, USA.

<sup>4</sup>Personal Health, 16/17 Rathgar Rd, Dublin, Dublin 6, Ireland

<sup>5</sup>Department of Mechanical Engineering, Technological University Dublin, Tallaght, Dublin, Ireland.

<sup>6</sup>Department of Psychology, Beaumont Hospital, Dublin 9, Ireland.

<sup>7</sup>Academic Unit of Neurology, Room 5.41, Biomedical Sciences Institute, Trinity College Dublin, Dublin 2, Ireland.

<sup>8</sup>Department of Neuropathology, Beaumont Hospital, Dublin 9, Ireland.

<sup>9</sup>Department of Neurosurgery, Stanford University School of Medicine, Stanford, California, USA.

<sup>10</sup>Department of Cognitive and Brain Sciences, Zlotowski Center for Neuroscience, Ben-Gurion University of the Negev, Beer-Sheva, 8410501 Israel.

<sup>11</sup>Department of Medical Neuroscience, Dalhousie University, Halifax, NS B3H 4R2, Canada.

<sup>12</sup>Department of Medicine, University College Cork, Cork, Ireland.

<sup>13</sup>Department of Radiology, St James’s Hospital, Dublin 8, Ireland.

<sup>§</sup>These authors contributed equally

\* To whom correspondence should be addressed

**Dr. Matthew Campbell**

Phone: **353 1 8961482**

Fax: **353 1 8963848**

Email: [Matthew.Campbell@tcd.ie](mailto:Matthew.Campbell@tcd.ie)

This paper has been peer-reviewed and accepted for publication, but has yet to undergo copyediting and proof correction. The final published version may differ from this proof.

**Dr Colin Doherty**

Phone: **353 1 4103688**

Fax: **353 1 4103477**

Email: [cpdoherty@stjames.ie](mailto:cpdoherty@stjames.ie)

## Abstract

While the diagnosis of moderate and severe TBI is readily visible on current medical imaging paradigms (MRI and CT scanning), a far greater challenge is associated with the diagnosis and subsequent management of mild TBI (mTBI), especially concussion which by definition is characterized by a normal CT.

To investigate whether the integrity of the blood-brain barrier (BBB) is altered in a high risk population for concussions, we studied professional mixed martial arts (MMA) fighters and adolescent rugby players. Additionally, we performed the linear regression between the BBB disruption defined by increased gadolinium contrast extravasation on dynamic contrast-enhanced (DCE-MRI) imaging on MRI and multiple biomechanical parameters indicating the severity of impacts recorded using instrumented mouthguards in professional MMA fighters. MMA fighters were examined pre-fight for a baseline and again within 120 hours post competitive fight, while rugby players were examined pre-season and again post-season or post-match in a sub-set of cases. DCE-MRI, serological analysis of BBB biomarkers, and an analysis of instrumented mouthguard data was performed.

Here, we provide pilot data that demonstrates disruption of the BBB in both professional MMA fighters and rugby players, dependent on the level of exposure. Our data suggest that biomechanical forces in professional MMA and adolescent rugby can lead to BBB disruption. These changes on imaging may serve as a biomarker of exposure of the brain to repetitive sub-concussive forces and mTBI.

## Introduction

Traumatic brain injury (TBI) is the leading cause of death in children and young adults globally. Indeed, the incidence of TBI can be considered to have reached epidemic proportions and there have been few recent advances for the treatment of malignant brain swelling that may evolve after severe TBI (1, 2). If brain swelling persists, the risks of permanent brain damage or mortality are greatly increased (3). While head injury is a relative risk in modern contact sports, the number of deaths and major disabilities originating from sports related severe TBI are small. A far greater challenge is the occurrence of repetitive mild TBI (mTBI), commonly referred to as concussive or sometimes sub-concussive injuries (4).

Generally, mTBI can be classified as injury to the brain resulting from blunt trauma or acceleration/deceleration of the head and neck with one or more of the following conditions attributable to the head injury during the post-traumatic surveillance period: **1)** Any period of observed or self-reported transient confusion, disorientation, or impaired consciousness; **2)** Any period of observed or self-reported dysfunction of memory (amnesia) around the time of injury; **3)** Observed signs of other neurological or neuropsychological dysfunction, such as seizures in the immediate aftermath of head injury, headache, dizziness, irritability, fatigue, or poor concentration (5).

In the context of participation in contact sports, there are frequently challenges in getting an accurate diagnosis and appropriate treatment post-concussion, especially when there is no documented or observed loss of consciousness or symptom complex that is easily recognised. Additionally, it must be recognized that there does not need to be any subjective clinical signs or symptoms for a brain injury to have occurred. In that regard, the nature of certain sports such as American football, rugby and boxing are such that repetitive exposure of the head to what is termed, sub-concussive forces, may lead to an accumulation of silent damage to distinct brain regions (6, 7, 8). However, current acute standard of care imaging with MRI is often not sensitive enough to pick up any damage and the underlying pathophysiology of these sub-concussive forces is far from established in human mTBI. Similarly, imaging paradigms following chronic exposure to mTBI is faced with similar challenges.

The exposure of children and young adults to sports that involve an increased risk of head trauma is controversial. We do know that boxing fighters suffer repeated mTBI episodes and are at risk of permanent brain damage and chronic traumatic encephalopathy (CTE) (9, 10). Although CTE is well known to be present in fighters and other professional contact athletes, there is far less data on the risks for children in contact sports (11)

We and others recently reported for the first time that blood-brain barrier (BBB) dysfunction is associated with pathology of CTE (12, 13). The BBB plays a critical role in maintaining central nervous system (CNS) homeostasis (14). Such is the impact of the BBB on neural integrity that it can be estimated that each neuron is perfused by its own capillary, with no neuron being further than  $\sim 25 \mu\text{m}$  from a capillary. Indeed, the combined surface area of cerebral microvessels is  $150\text{-}200 \text{ cm}^2/\text{g}$  of brain tissue which equates to approximately  $15\text{-}20 \text{ m}^2$  per adult human brain (15, 16, 17, 18).

Given that BBB integrity is readily assessed in human subjects, we have sought to understand the character, mechanism, and structural/functional consequences of exposure to head impacts in two age groups. We prospectively followed professional mixed martial arts (MMA) fighters and adolescent rugby union players

Surprisingly, we found evidence of dynamic BBB disruption in a sub-set of adolescents exposed to a season (6 months) of rugby union in the absence of diagnosed concussion. This disruption was measured with enhanced gadolinium signal and occurred in tandem with a distinct set of serological, readouts that may allow for an objective measure of neural damage to be assessed. In five professional MMA fighters who were all diagnosed with a concussion, we observed a wide spectrum of BBB integrity. Using well-established instrumented mouthguard technology in the fighters, the linear regression between the mechanical parameters indicating the severity of the impacts and the resultant BBB disruption were performed. Some of the parameters show good correlations, which suggested a potential means of assessing damage to the concussed brain.

## Results

### BBB disruption is linked to repetitive head trauma

Using instrumented mouthguard technology (outlined in full in methods section), we established a link between single and repetitive head impacts and BBB disruption (**Fig 1**). We recruited five professional MMA fighters to undergo pre-fight and post-fight testing and imaging (**Fig 1c, d**). In combination, we instrumented the participants to measure head impact severity and exposure during fights (**Fig 1a**). The number of impacts and the kinematics of these impacts were found to be in linear correlation to the volume fraction (**Fig.1f, g, h**). We also used finite element (FE) modelling to estimate brain tissue deformation produced by the head impacts (**Fig 1c**). To find the most sensitive mechanical parameters to BBB disruption, the 1<sup>st</sup> principal strain ( $\epsilon$ ), 1<sup>st</sup> principal strain rate ( $\dot{\epsilon}$ ), 1<sup>st</sup> principal stress ( $\sigma$ ) and the power absorbed ( $\omega$ ) were extracted from the simulation results. Considering the amplitude, the duration and the repeatability of the strike may contribute to BBB disruption. Various methods, detailed in the Methods section, were used to calculate parameters to indicate the severity of all impacts. The results were correlated to the average slopes of contrast intensity and the fraction of volume where the BBB was disrupted, as shown in **Table.1**. Some of the linear regressions were plotted in **Fig.1i-q**. For our cohort,  $\epsilon_x^1$ ,  $\epsilon_y^1$ ,  $\sigma_z^1$  were in good correlation with both the average slope and the BBB disruption volume fraction, and the  $\epsilon_x^p$ ,  $\epsilon_y^p$  were only in good correlation with the BBB disruption volume fraction ( $R^2 > 0.80$ ). However, considering only 6 data points were used in regression, these correlations need to be validated in the future. All parameters relating to the power/energy were found to be poorly correlated to disruption of BBB. The maps of  $\epsilon^p$  were compared with the maps of BBB disruption locally (**Fig.1c**), however, the increased deformation was not locally associated with the increased changes of BBB.

**Table.1**  $R^2$  of the linear regression between brain deformation and BBB disruption. (The color indicates the  $R^2$ , white is corresponding to  $R^2 = 0$  and red is corresponding to  $R^2 > 0.8$ )

	Points Time	Average BBB Disruption (Slope)			Volume Fraction of BBB Disruption		
		Total, $\Sigma$	Average, A	95%Max, 95	Total, $\Sigma$	Average, A	95%Max, 95
<b>1st Principal Strain, <math>\epsilon</math></b>	Integration, I	0.81	0.44	0.38	0.89	0.53	0.46
	Peak, P	0.64	0.29	0.28	0.84	0.50	0.52
<b>1st Principal Strain Rate, <math>\dot{\epsilon}</math></b>	Integration, I	0.84	0.52	0.56	0.96	0.68	0.74
	Peak, P	0.60	0.28	0.29	0.82	0.49	0.52
<b>1st Principal Stress, <math>\sigma</math></b>	Integration, I	0.80	0.37	0.46	0.96	0.56	0.70
	Peak, P	0.42	0.20	0.23	0.53	0.29	0.29
<b>Power Absorbed, <math>\omega</math></b>	Integration, I	0.23	0.20	0.19	0.25	0.22	0.20
	Peak, P	0.18	0.18	0.17	0.19	0.18	0.17

### BBB disruption is evident in rugby players post-season

Using a weight-based bolus injection of Gadolinium and a dynamic contrast enhanced MRI (DCE-MRI) paradigm (19), we were able to measure BBB integrity in rugby players examined pre-season (before regular full contact training and competition) and again at a return imaging session following conclusion of the rugby season (**Fig 2a**). With a sample size of 19, there were no overall differences in gadolinium signal when pre-season scans were compared to post-season scans across the entire group (**Fig 2b**). However, increases in signal post-season when compared to pre-season were observed in the periventricular regions of the brain in 10 of 19 subjects who completed the study (**Fig 2c**). Indeed, when the BBB disrupted voxels across the entire groups were examined at pre-season compared to post-season, it was evident that a sub-group of individuals displayed increased BBB disruption post-season compared to their pre-season scan (**Fig 2d**). This BBB disruption was significantly increased in this sub-group of players (**Fig 2e**)

Systemic biomarkers of BBB damage and brain trauma have been purported to have utility in determining prognosis post TBI. In this regard, we screened plasma samples from participants pre- and post-season in an effort to examine the differential expression of 14 common "TBI biomarkers". Of these (outlined in full in methods section), only 2 were detectable at sufficiently high levels to be quantified. Levels of brain derived neurotrophic factor (BDNF) (**Fig 2f**) were significantly increased in subjects post-season compared to

plasma levels pre-season (\*\*P = 0.004). No differences were observed in levels of monocyte chemotactic protein (MCP-1) (**Fig 2g**). Levels of the commonly used BBB disruption biomarker, S100B, surprisingly decreased in plasma samples post-season compared to pre-season (\*P < 0.05) (**Fig 2h**). There was only a very weak correlation of S100B levels with the % disrupted voxels, but this was a negative correlation (**Fig S1**).

### **BBB disruption in the acute stages post-match**

While BBB disruption and differential levels of biomarkers were evident in analyses of pre-season versus post-season schoolboy rugby players, we wished to ascertain whether this BBB disruption was occurring in the acute phases post exposure to repetitive head trauma. In this regard, we recruited a sub-group of university-based rugby union players (aged 18-23). In this group, we enrolled 8 participants to undergo pre-season testing and imaging. Using the linear method of DCE-MRI analysis, 2 out of 8 subjects had an increased signal intensity post match compared to their pre-season scan (**Fig 3a**) one of which returned to baseline at the end of the season (**Fig 3c**), showing reversibility of the BBB disruption, while the other manifested a higher signal post season.

Unlike the pre-season/post-season analyses, examining levels of BDNF in participants did not show any difference in plasma levels post-match compared to pre-season (**Fig 3c**), however, levels of MCP-1 were significantly increased post-match in this group (\*P = 0.012) (**Fig 3d**). Interestingly, and as has been reported previously, S100B levels were also shown to increase significantly post-match (\*P = 0.01) (**Fig 3e**). There was weak positive correlation between S100B levels and % disrupted voxel increases (**Fig S1**). The demographic of rugby players and MMA fighters who participated in our study is outlined in **Fig. S2**.

### **Discussion**

Our pilot study provides the first analysis of BBB function in a group of MMA fighters and rugby players exposed to varying levels of repetitive head trauma in the context of playing competitive contact sports. Taken together, our data suggest that dynamic changes to the BBB may occur after a full season of contact sport with these changes manifesting in up to 52 % of adolescents. While there were slight modifications to the MRI scanning parameters between the schoolboy rugby study and the university rugby study/MMA study, we observed no significant differences between the values generated. Additionally,

the pattern of BDNF, MCP-1 and S100B, biomarkers detected post-season and post-match, suggest that these markers may aid in the indication of sub-concussive trauma, and possibly also inform in return to baseline assessments. Importantly however, it appears that these biomarkers may have limited utility as “stand-alone” readouts as we observed decreased levels of S100B in bloods of players after a full season of rugby. The elusive temporal profile of these biomarkers after trauma also make it challenging to use solely as a biomarker of brain injury.

From animal TBI models, it is suggested that TBI may cause primary damage to the brain parenchyma leading to BBB pathophysiology and CTE (13, 20). From the field of ultrasound assisted drug delivery, it is well known that mechanical forces open the BBB complex in humans and result in inflammation. However, animal studies do not necessarily recapitulate the tissue level biomechanical forces experienced by humans in sports, so it is unknown if BBB disruption and inflammation occur in child or adult athletes. In this regard, in our study we measured the kinematics and the severity of head hits sustained by five professional MMA fighters who also underwent pre-fight and post-fight testing and imaging in six fights (**Fig 1**). Although all five fighters were concussed, we found a wide spectrum of BBB integrity. Based on this pilot data, we found  $\epsilon_{\Sigma}^1$ ,  $\dot{\epsilon}_{\Sigma}^1$ ,  $\sigma_{\Sigma}^1$ ,  $\epsilon_{\Sigma}^P$ ,  $\dot{\epsilon}_{\Sigma}^P$ ,  $\epsilon_{95}^1$ ,  $\sigma_{95}^1$  were correlated to the disruption of the BBB well, indicating these parameters could be potential candidates to induce the dysfunction. However, owing to the different geometry and the low resolution of FE head model, the maps of the mechanical parameter could not be associated with the BBB disruption locally. In the subject who was knocked out within the first 2 minutes of the fight (**Fig 1c**, **Fight 3**), we found little evidence of BBB disruption even after a transient loss of consciousness. However, upon inspecting the mouthguard data, we found relatively low accelerations (four impacts all less than 50 gs and 5000 rad per second squared) and small brain strains from FE modelling (less than 10% maximum principal strain). Although the study sample is too small for conclusive findings, and cumulative effect of the multiple impact is not considered, this research supports the hypothesis that repetitive head impacts may cause BBB disruption. The simultaneous correlation of severity of hits we observed in concussed professional fighters leaves open the question as to what effect repetitive sub-concussive exposure may have on its own.

In the context of moderate or severe TBI, it is known that BBB disruption is an early event that can persist for years and decades after the initial injury (21, 22). It is of major interest that the end stage pathology observed in CTE appears to be a terminal disruption and dysfunction in the integrity of the BBB in areas of dense perivascular P-Tau deposition (11). In CTE, it is tempting to suggest that repetitive exposure to head trauma, as observed in a subset of players in our study, without allowing sufficient time BBB recovery, will lead to long term and persistent BBB disruption and therefore to the long-term sequelae associated with some forms of mTBI (23, 24). In animal studies, such prolonged BBB disruption is associated with neuroinflammation and pathological synaptogenesis, plasticity and hence abnormal network activity (13).

While our study cannot speak pervasively to concussive brain injuries *per se*, we have highlighted that the very nature of contact sports as violent as MMA and as typical as rugby can manifest dynamic changes to the integrity and regulation of the BBB due to what we can term “sub-concussive” events.

The current clinical assessment of mTBI falls far below the kind of objective criteria that would provide meaningful and clinically robust diagnostic and prognosis information for patients. This is compounded not only by the lack of an appropriate imaging paradigm but also due to the lack of any systemic biomarkers that can predict the severity of injury. Lately, there has been a growing awareness of implications of concussive brain injuries in sports given the well-defined increased risk of dementia associated with moderate or severe TBI (26, 27, 28, 29) and emerging evidence suggestive of a link between repetitive mild head trauma and the development of CTE (30, 31, 32). There is a clear need for understanding the molecular aetiology of concussive and sub-concussive brain injuries and for developing methods to aid in the diagnosis and management of such injuries to the brain.

While participation in sports activities is hugely important for social, physiological and psychological development of children and young adults, it is critical that we make objective and rational decisions on a case-by-case basis when deciding whether athletes should compete in full contact sports. The most common contact sports include rugby, American football, boxing, horse riding and MMA. What remains to be elucidated, however, is whether these sports are putting future brain health at an acceptable risk.

Expanded and longitudinal studies using the multidisciplinary methods outlined in the current pilot study will undoubtedly lead to better management and clinical decision making with regard to repetitive mTBI. Imaging of BBB integrity in tandem with serological analysis of participants in contact sports could also form the central platform in diagnosis and may better inform return to play guidelines.

## Methods

### Head impact measurements and brain tissue deformation estimations

We deployed the Stanford Instrumented Mouthguard (MiG2.0) to 5 professional MMA fighters during regular matches (n=5 subjects, 6 fights). The human subject protocol was approved by the Stanford, Trinity College and Institute of Technology Tallaght Panel for the Protection of Human Subjects. We conducted data collection in accordance with the institutional review boards' guidelines and regulations. Both video analysis and instrumented mouthguard data were used to validate each impact.

The MiG2.0 senses 6 degree of freedom kinematics via a triaxial accelerometer and a triaxial gyroscope. The sensory board is completely sealed between three layers of ethylene vinyl acetate (EVA) material and communication occurs via blue-tooth. A tight fit to the dentition is achieved by forming the EVA material around a dental model (33). In this study we recorded events with linear acceleration exceeding 10 g in agreement with previously published systems (34). The acquisition window was 50 ms pre-trigger and 150 ms post-trigger. Linear acceleration and angular velocity were filtered using a 4th order Butterworth low-pass filter with cut-off frequency of 300Hz. Angular acceleration was estimated using a 5-point stencil derivative of the measured angular velocity.

Estimates of brain tissue deformation for all head impacts were obtained from simulations using the KTH finite element (FE) model (KTH Royal Institute of Technology, Stockholm, Sweden) (35, 36). This model includes the brain, skull, scalp, meninges, cerebrospinal fluid (CSF), and 11 pairs of bridging veins. Skull acceleration measured from the MiG2.0 was prescribed to follow the measured 6DOF head accelerations and ensuing brain deformation was observed. The brain was modelled as an Ogden hyper-elastic constitutive material to account for large deformations of the tissue, with additional linear viscoelastic terms to account for the rate dependence of the tissue. The boundary condition between the dura and skull was tied. Between the brain and dura, a sliding

interface was implemented that allowed tangential, and not radial, movement between the structures (given the incompressibility of the mostly-water CSF). The determined brain geometry and material properties were validated against displacement data from cadaver head impact experiments where neutral density targets were inserted inside cadaver brains and tracked using high-speed biplane X-ray during impacts (37, 38).

To locally compare brain deformation to BBB disruption from DCE-MRI images we implemented a protocol involving FE mesh voxelization and an affine registration between the DCE brain mask and the voxelized FE brain mask. Firstly, the FE brain mesh was voxelized to obtain a reference volume (MATLAB R2018a); subsequently a spatial transformation was used to align the DCE-MRI brain to the model. The volume resampling was performed with the 3D SLICER 4.10.0 BRAIN registration package. Based on spatial coordinates, the mechanical deformation was assigned to the DCE-MRI voxels belonging to the corresponding element, and only the voxels with the BBB disruption were considered in the linear regression. Different methods were used to calculate a scalar quantity to represent the severity of brain deformation during the game. As an example shown in **Eq.1**, the peak (superscript P) and the integration (superscript I) over history of the strain ( $\epsilon$ ), the strain rate ( $\dot{\epsilon}$ ), the stress ( $\sigma$ ) and the power absorbed ( $\dot{a}$ ) were calculate for every point and impact. Then, the effect of the multiple impact is considered and the maximum values over all impact were calculated for every points. The values for points in the map were caused by different impacts. The Total ( $\Sigma$ ), average (A) and the value which was higher than that in 95% points (95) were calculated and used in the regression.

$$\epsilon_{\Sigma}^I = \Sigma_{(x,y,z)} \left( \text{Maximum}_{im} \left( \int_t \epsilon(t, im, x, y, z) \cdot dt \right) \right) \quad \text{Eq.1}$$

Where  $\epsilon(t, im, x, y, z)$  is the strain at point  $(x, y, z)$ , at time point  $t$ , in the impact  $im$ . The maximum peak values of the magnitude of linear ( $a$ ) and angular ( $\beta$ ) acceleration were calculated as an example shown in Eq.2.

$$\alpha^P = \text{Maximum}_{im} \left( \text{Maximum}_t (a) \right) \quad \text{Eq.2}$$

### Magnetic Resonance Imaging (MRI)

All ethical approvals were in place prior to initiation of studies on human subjects. Initially, 22 participants were recruited pre-season for the schoolboy study, however only 11 returned for post-season evaluation. All participants underwent a pre-season scan prior to

the start of the competitive rugby season and underwent a post season scan within two months of the end of the season in the case of the schoolboy team ( $n = 11$ ). In addition, the university-based team participants (Initially  $n = 10$  recruited but only  $n = 8$  were scanned post match) underwent a scan within 2 hours of playing a full contact competitive rugby match. BBB permeability maps were created using the slope of contrast agent concentration in each voxel over time, calculated by a linear fit model as previously described. Thresholds of high permeability was defined by the 95<sup>th</sup> percentile of all slopes in a previously examined control group (39). Supra-threshold values of individuals were then normalized to pre-season values to determine relative change over the course of play. MMA fighters were scanned pre-fight and again within 120 hours post competitive fight using identical parameters as that used in the university-based rugby players.

All imaging was performed using a 3T Philips Achieva scanner, and included a T1-weighted anatomical scan (3D gradient echo, TE/TR = 3/6.7 ms, acquisition matrix 268x266, voxel size: 0.83x0.83x.9mm), T2-weighted imaging (TE/TR = 80/3000 ms, voxel size: 0.45x0.45x.4mm), FLAIR (TE/TR = 125/11000 ms, voxel size: 0.45x0.45x4mm).

In the first cohort, the calculation of pre-contrast longitudinal relaxation time ( $T_{10}$ ), the variable flip angle (VFA) method was used (3D T1w-FFE, TE/TR = 2.78/5.67 ms, acquisition matrix: 240x184, voxel size: 0.68x0.68x5 mm, flip angles: 2,10,16 and 24°). Dynamic contrast enhanced (DCE) sequence was then acquired (Axial, 3D T1w-FFE, TE/TR = 2.78/5.6 ms, acquisition matrix: 240x184, voxel size: 0.68x0.68x5 mm, flip angle: 6°,  $\Delta t = 6.5$  Sec, temporal repetitions: 70, total scan length: 7.6 minutes). An intravenous bolus injection of the contrast agent gadobentate dimeglumine (Gd-BOPTA, Bracco Diagnostics Inc., Milan, Italy) was administered using an automatic injector after the first three DCE repetitions.

For the second, older cohort, T1-weighted, T2-weighted and FLAIR imaging parameters were kept the same. For the calculation of pre-contrast longitudinal relaxation time ( $T_{10}$ ), the variable flip angle (VFA) method was used (3D T1w-FFE, TE/TR = 2.78/5.67 ms, acquisition matrix: 208x,204 voxel size: 0.86x0.86x6 mm, flip angles: 10,15, 20, 25 and 30°). Dynamic contrast enhanced (DCE) sequence was then acquired (Axial, 3D T1w-FFE, TE/TR = 2.78/5.6 ms, acquisition matrix: 208x,204 voxel size: 0.86x0.86x6 mm, flip angle: 20°,  $\Delta t = 22.2$  Sec, temporal repetitions: 61, total scan length: 22.6 minutes). Intravenous bolus

injection of the contrast agent gadobentate dimeglumine was administered using an automatic injector after the first five DCE repetitions.

To obtain permeability values in healthy individuals, we (Co-author, Prof Alon Friedman's group) first scanned a cohort of 27 non-contact sport athletes ( $n=27$  males, range, 18-36 years; median, 28 years). Each registered brain voxel was assigned a value corresponding to a *normalized permeability*. Based on a cumulative distribution function (CDF) of normalized permeability values, we defined an upper limit for "normal" permeability as the 95<sup>th</sup> percentile of the mean CDF. Brain voxels with higher values were considered as having "*abnormally high permeability*". An additional control group (healthy, non-athlete controls) recruited at a later stage ( $n = 26$ , range 18-40, median, 30 years) as a test group. No differences in permeability maps were found between the two separate control groups.

Changes in DCE scan length were made as the shorter scan time can sometimes inflate the LDM signal, as the length of time allowed for the contrast signal to decay following bolus injection until scan completion is less. To align scans with a previous study (34) a longer scan time was utilised in the university rugby cohort and the MMA cohort. The values measured were normalised to an internal ROI and therefore relative values are used to generate % voxels. Also, there was no significant difference between the values generated using the shortened scan time and the longer scan time.

### **Human plasma analyses**

Immediately prior to under-going an MRI scan, 16 ml of whole blood was withdrawn in K<sub>2</sub> EDTA-coated tubes. Plasma and Peripheral Blood Mononuclear Cell (PBMC) fractions were separated by density fractionation. Briefly, whole blood samples were diluted 1:1 with PBS prior to being layered on to 10 ml of Lymphoprep (Stemcell Technologies, Vancouver, Canada). Samples were centrifuged at 400 G for 45 mins with 0 acceleration and deceleration to separate blood into plasma and PBMC fractions and stored at -80°C until use.

Plasma BDNF, MCP-1/CCL2 and S100B levels were measured using the Xmap (Luminex) method (R&D Systems, Minneapolis, USA) and ELISA (R&D Systems, Minneapolis, USA) per the manufacturer's instructions. In brief, the Luminex platform (consisting of the following analytes: BDNF, MCP-1/CCL2, S100B, IL-6, IL-18, IL-1Beta, IL-33, IL-17A, IL-12 p70, IL-23,

TGF-Alpha, T-Tau, IFN- Gamma and GFAP) involved incubating diluted plasma samples (50  $\mu$ l) in a 96-well plate containing antibody coated magnetic beads for 2 hours at room temperature with gentle orbital agitation. After incubation, the beads were washed with the provided wash buffer and signal developed using the provided biotin antibody cocktail and streptavidin-peroxidase. Signal was determined using a Luminex 200 plate reader. Importantly, only levels of BDNF, MCP-1/CCL2 and S100B could be detected at sufficiently high levels and were subsequently chosen to confirm levels of expression using ELISA analysis.

For samples analysed using ELISA, plasma samples were incubated in individual 96-well plates coated with capture antibodies to human BDNF, MCP-1/CCL2 and S100B for 2 hours at room temperature with gentle horizontal agitation. After incubation, plates were washed with the wash buffer and signal developed using the provided biotin labelled antibody and streptavidin-peroxidase. Signal was determined using an ELISA plate reader. Levels of BDNF, MCP-1/CCL2 and S100B were calculated by a standard curve for each analyte. In 2 samples collected, haemolysis was present during collection and these were excluded from analysis.

### **Statistical Analyses**

Statistical analysis was performed using Student's t-test, with significance represented by a P value of  $\leq 0.05$ . For multiple comparisons, ANOVA was used with a Tukey-Kramer post-test and significance represented by a P value of  $\leq 0.05$ . ANOVA followed by a Bonferroni post-test was used for multiple comparisons was used with  $P \leq 0.05$  representing significance. G\*Power was used a priori to calculate an appropriate sample size to ensure adequate power for experiments. For biomechanical regression with DCE-MRI results, multiple comparisons were made to look for correlations. Therefore, statistical significance is not considered in this analysis.

### **Acknowledgments**

This work was supported by grants from Science Foundation Ireland (SFI), (12/YI/B2614 and 11/PI/1080), The Health Research Board of Ireland (HRB), the BrightFocus Foundation, the St James' Hospital Foundation with support to EK from the Ellen Mayston Bates Bequest at the Trinity Foundation. The Campbell lab at TCD is also supported by an SFI

Centres grant supported in part by a research grant from SFI under grant number 16/RC/3948 and co-funded under the European Regional Development fund by FutureNeuro industry partners. Work in the laboratory of AF is supported by the Canada Institute for Health Research (CIHR) (AF). We thank Caroline Woods and Charles Murray for animal husbandry.

### **Conflict of Interest Statement**

The authors declare no conflict of interest.

### **Author Contributions**

EOK: Analysed MRI data. EK: Performed clinical work-up of participants. CG: Performed instrumented mouthguard analysis. EW and AH: Performed clinical work-up of participants. CG: Analysed data. ST and AM: Performed instrumented mouthguard analysis. SH: Data collection. TB: Analysed data. JK: data collection ND: Data collection. GAG: MRI analysis and design. AF: MRI analysis and design. RV: MRI analysis and design. MGM: Conceived experiments. JFM: Conceived MRI experiments. NP: Conceived experiments. DC: Performed instrumented mouthguard analysis. CD: Conceived, designed and performed experiments, analysed data and wrote the paper. MC: Conceived, designed and performed experiments, analysed data and wrote the paper.

### **Author Disclosure Statement**

Authors declare no conflicts of interest

## References

1. Bob Roozenbeek, Andrew I. R. Maas & David K. Menon. Changing patterns in the epidemiology of traumatic brain injury. *Nature Reviews Neurology* 9, 231-236 (2013).
2. Helmy A, Vizcaychipi M, Gupta AK. Traumatic brain injury: intensive care management. *Br J Anaesth.* 2007 Jul; 99(1):32-42.
3. Stokum JA, Gerzanich V, Simard JM. Molecular pathophysiology of cerebral edema. *J Cereb Blood Flow Metab.* 2016 Mar;36(3):513-38.
4. Montenigro PH, Alosco ML, Martin BM, Daneshvar DH, Mez J, Chaisson CE, Nowinski CJ, Au R, McKee AC, Cantu RC, McClean MD, Stern RA, Tripodis Y. Cumulative Head Impact Exposure Predicts Later-Life Depression, Apathy, Executive Dysfunction, and Cognitive Impairment in Former High School and College Football Players. *J Neurotrauma.* 2017 Jan 15;34(2):328-340.
5. McCrory P, Meeuwisse W, Dvorak J, Aubry M, Bailes J, Broglio S, Cantu RC, Cassidy D, Echemendia RJ, Castellani RJ, Davis GA, Ellenbogen R, Emery C, Engebretsen L, Feddermann-Demont N, Giza CC, Guskiewicz KM, Herring S, Iverson GL, Johnston KM, Kissick J, Kutcher J, Leddy JJ, Maddocks D, Makdissi M, Manley GT, McCrea M, Meehan WP, Nagahiro S, Patricios J, Putukian M, Schneider KJ, Sills A, Tator CH, Turner M, Vos PE. Consensus statement on concussion in sport-the 5th international conference on concussion in sport held in Berlin, October 2016. *Br J Sports Med.* 2017 Apr 26
6. Lynall RC, Campbell KR, Wasserman EB, Dompier TP, Kerr Z. Concussion mechanisms and activities in youth, high school, and college football. *J Neurotrauma.* 2017 May 10.
7. McMillan TM, McSkimming P, Wainman-Lefley J, Maclean LM, Hay J, McConnachie A, Stewart W. Long-term health outcomes after exposure to repeated concussion in elite level: rugby union players. *J Neurol Neurosurg Psychiatry.* 2017 Jun;88(6):505-511
8. Purcell LK, Leblanc CM; Canadian Paediatric Society, Healthy Active Living and Sports Medicine Committee, and American Academy of Pediatrics, Council on Sports Medicine and Fitness. Boxing participation by children and adolescents: A

- joint statement with the American Academy of Pediatrics. *Paediatr Child Health*. 2012 Jan;17(1):39-40.
9. Koerte IK, Nichols E, Tripodis Y, Schultz V, Lehner S, Igbinoba R, Chuang AZ, Mayinger M, Klier EM, Muehlmann M, Kaufmann D, Lepage C, Heinen F, Schulte-Körne G, Zafonte R, Shenton ME, Sereno AB. Impaired Cognitive Performance in Youth Athletes Exposed to Repetitive Head Impacts. *J Neurotrauma*. 2017 Jun 9.
  10. Mez J, Solomon TM, Daneshvar DH, Murphy L, Kiernan PT, Montenigro PH, Kriegel J, Abdolmohammadi B, Fry B, Babcock KJ, Adams JW, Bourlas AP, Papadopoulos Z, McHale L, Ardaugh BM, Martin BR, Dixon D, Nowinski CJ, Chaisson C, Alvarez VE, Tripodis Y, Stein TD, Goldstein LE, Katz DI, Kowall NW, Cantu RC, Stern RA, McKee AC. Assessing clinicopathological correlation in chronic traumatic encephalopathy: rationale and methods for the UNITE study. *Alzheimers Res Ther*. 2015 Oct 12;7(1):62.
  11. Smith DH, Johnson VE, Trojanowski JQ, Stewart W. Chronic traumatic encephalopathy - confusion and controversies. *Nat Rev Neurol*. 2019 Jan 21.
  12. Doherty CP, O'Keefe E, Wallace E, Loftus T, Keaney J, Kealy J, Humphries MM, Molloy MG, Meaney JF, Farrell M, Campbell M. Blood-Brain Barrier Dysfunction as a Hallmark Pathology in Chronic Traumatic Encephalopathy. *J Neuropathol Exp Neurol*. 2016 Jul;75(7):656-62.
  13. Tagge CA, Fisher AM, Minaeva OV, Gaudreau-Balderrama A, Moncaster JA, Zhang XL, Wojnarowicz MW, Casey N, Lu H, Kokiko-Cochran ON, Saman S, Ericsson M, Onos KD, Veksler R, Senatorov VV Jr, Kondo A, Zhou XZ, Miry O, Vose LR, Gopaul KR, Upreti C, Nowinski CJ, Cantu RC, Alvarez VE, Hildebrandt AM, Franz ES, Konrad J, Hamilton JA, Hua N, Tripodis Y, Anderson AT, Howell GR, Kaufer D, Hall GF, Lu KP, Ransohoff RM, Cleveland RO, Kowall NW, Stein TD, Lamb BT, Huber BR, Moss WC, Friedman A, Stanton PK, McKee AC, Goldstein LE. Concussion, microvascular injury, and early tauopathy in young athletes after impact head injury and an impact concussion mouse model. *Brain*. 2018 Feb 1;141(2):422-458.
  14. Abbott NJ, Patabendige AA, Dolman DE, Yusof SR, Begley DJ. (2010) Structure and function of the blood-brain barrier. *Neurobiol Dis*. 37(1):13-25.

15. Abbott NJ, Ronnback L, Hansson E. (2006) Astrocyte-endothelial interactions at the blood-brain barrier. *Nat Rev Neurosci* 7(1):41-53.
16. Pardridge WM. (2005) The blood-brain barrier: bottleneck in brain drug development. *NeuroRx* 2(1):3-14.
17. Hawkins BT, Davis TP. (2005) The blood-brain barrier/neurovascular unit in health and disease. *Pharmacol Rev* 57(2):173-85.
18. Obermeier B, Daneman R, Ransohoff RM. (2013) Development, maintenance and disruption of the blood-brain barrier. *Nat Med.* 19(12):1584-96.
19. Veksler R, Shelef I, Friedman A. Blood-brain barrier imaging in human neuropathologies. *Arch Med Res.* 2014 Nov;45(8):646-52.
20. Johnson VE, Weber MT, Xiao R, Cullen DK, Meaney DF, Stewart W, Smith DH. Mechanical disruption of the blood-brain barrier following experimental concussion. *Acta Neuropathol.* 2018 May;135(5):711-726.
21. Hay JR, Johnson VE, Young AM, Smith DH, Stewart W. Blood-Brain Barrier Disruption Is an Early Event That May Persist for Many Years After Traumatic Brain Injury in Humans. *J Neuropathol Exp Neurol.* 2015 Dec;74(12):1147-57.
22. Doherty CP, O'Keefe E, Keaney J, Lawlor B, Coen RF, Farrell M, Campbell M. Neuropathology as a result of severe traumatic brain injury? *Clin Neuropathol.* 2019 Jan/Feb;38(1):14-22
23. Greene, C, Kealy, J, Humphries, MM, Gong, Y, Hou, J, Hudson, N, Cassidy, LM, Martiniano, R, Shashi, V, Hooper, SR, Grant, GA, Kenna, PF, Norris, K, Callaghan, CK, Islam, MN, O'Mara, SM, Najda, Z, Campbell, SG, Pachter, JS, Thomas, J, Williams, NM, Humphries, P, Murphy, KC and Campbell, M. Dose dependent expression of claudin-5 is a modifying factor in schizophrenia. *Molecular Psychiatry*, 2017, 2017, Oct 10.
24. Menard C, Pfau ML, Hodes GE, Kana V, Wang VX, Bouchard S, Takahashi A, Flanigan ME, Aleyasin H, LeClair KB, Janssen WG, Labonté B, Parise EM, Lorsch ZS, Golden SA, Heshmati M, Tamminga C, Turecki G, Campbell M, Fayad ZA, Tang CY, Merad M, Russo SJ. Social stress induces neurovascular pathology promoting depression. *Nat Neurosci.* 2017 Dec;20(12):1752-1760.

25. Nitta T, Hata M, Gotoh S, Seo Y, Sasaki H, Hashimoto N, *et al.* (2003) Size-selective loosening of the blood-brain barrier in claudin-5-deficient mice. *J Cell Biol.* 161(3):653-60.
26. Ojo JO, Mouzon B, Algamal M, Leary P, Lynch C, Abdullah L, Evans J, Mullan M, Bachmeier C, Stewart W, Crawford F. Chronic Repetitive Mild Traumatic Brain Injury Results in Reduced Cerebral Blood Flow, Axonal Injury, Gliosis, and Increased T-Tau and Tau Oligomers. *J Neuropathol Exp Neurol.* 2016 Jul;75(7):636-55.
27. Mortimer JA, van Duijn CM, Chandra V, Fratiglioni L, Graves AB, Heyman A, Jorm AF, Kokmen E, Kondo K, Rocca WA. Head trauma as a risk factor for Alzheimer's disease: a collaborative re-analysis of case-control studies. EURODEM Risk Factors Research Group. *Int J Epidemiol.* 1991;20:S28–S35.
28. Fleminger S, Oliver DL, Lovestone S, Rabe-Hesketh S, Giora A. Head injury as a risk factor for Alzheimer's disease: the evidence 10 years on; a partial replication. *J Neurol Neurosurg Psychiatry.* 2003 Jul;74(7):857-62.
29. Gardner RC, Burke JF, Nettiksimmons J, Kaup A, Barnes DE, Yaffe K. Dementia risk after traumatic brain injury vs nonbrain trauma: the role of age and severity. *JAMA Neurol.* 2014 Dec;71(12):1490-7.
30. Stewart W, McNamara PH, Lawlor B, Hutchinson S, Farrell M. Chronic traumatic encephalopathy: a potential late and under recognized consequence of rugby union? *QJM.* 2016 Jan;109(1):11-5.
31. Iacono D, Shively SB, Edlow BL, Perl DP. Chronic Traumatic Encephalopathy: Known Causes, Unknown Effects. *Phys Med Rehabil Clin N Am.* 2017 May;28(2):301-321.
32. McKee AC, Cairns NJ, Dickson DW, Folkerth RD, Keene CD, Litvan I, Perl DP, Stein TD, Vonsattel JP, Stewart W, Tripodis Y, Crary JF, Bieniek KF, Dams-O'Connor K, Alvarez VE, Gordon WA; TBI/CTE group. The first NINDS/NIBIB consensus meeting to define neuropathological criteria for the diagnosis of chronic traumatic encephalopathy. *Acta Neuropathol.* 2016 Jan;131(1):75-86.
33. Wu LC, Nangia V, Bui K, *et al* (2016) In Vivo Evaluation of Wearable Head Impact Sensors. *Ann Biomed Eng* 44:1234–1245.
34. Kuo C, Wu LC, Hammor BT, *et al* (2016) Effect of the mandible on mouthguard measurements of head kinematics. *J Biomech* 49:1845–1853.

35. Hernandez F, Wu LC, Yip MC, et al (2015) Six Degree-of-Freedom Measurements of Human Mild Traumatic Brain Injury. *Ann Biomed Eng* 43:1918–1934.
36. Kleiven S (2007) Predictors for traumatic brain injuries evaluated through accident reconstructions. *Stapp Car Crash J* 51:81–114.
37. Hardy W (2001) Investigation of head injury mechanisms using neutral density technology and high-speed biplanar x-ray. *Stapp Car Crash J* 45:337–368
38. Hardy WN, Mason MJ, Foster CD, et al (2008) A study of the response of the human cadaver head to impact. *Stapp Car Crash J* 51:17–80
39. Weissberg I, Veksler R, Kamintsky L, Saar-Ashkenazy R, Milikovsky DZ, Shelef I, Friedman A. Imaging blood-brain barrier dysfunction in football players. (2014) *JAMA Neurol.* Nov;71(11):1453-5.

## Figure legends

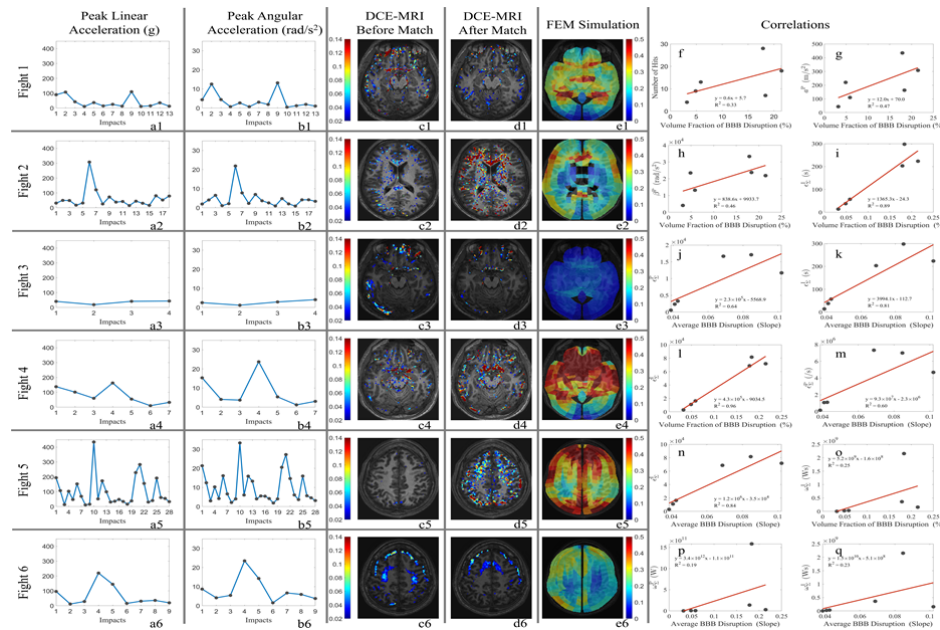


**Figure 1:** **a1-6)** Peak linear acceleration magnitude of the head measured by Stanford instrumented mouthguards (MiG 2.0) in professional mixed martial arts (MMA) fights 1-6 ( $n = 5$  individual fighters). **b1-6)** Peak angular acceleration magnitude of head measured by MiG 2.0 in professional mixed martial arts (MMA) fights 1-6. **c1-6)** Map of Blood Brain Barrier (BBB) disruption of the MMA fighters before the fights 1-6. **d1-6)** Map of BBB disruption of the MMA fighters after the matches 1-6. Both **c1-6)** and **d1-6)** were measured by DCE-MRI. **e1-6)** Map of peak deformation (1<sup>st</sup> principal strain) during the fight. The deformations were obtained by assigning the kinematics measured during the fights to the KTH head model. The maximum deformations were selected among all impacts for every element independently. **f)** Linear regression between the volume of BBB disruption (in %) and the total number of head impacts sustained during the fights. **g)** Linear regression between the volume of BBB disruption (in %) and the peak linear acceleration magnitude. **h)** Linear regression between the volume of BBB disruption (in %) and the peak angular acceleration magnitude. **i)** Linear regression between the volume of BBB disruption (in %) and the integration of total deformation (sum of the Green strain over all elements) in the fiercest impact (the impact in which the value maximizes). **j)** Linear regression between the average BBB disruption (expressed as slope) and the peak value of total deformation in the fiercest impact. **k)** Linear regression between the average

BBB disruption (expressed as slope) and the integration of total deformation in the fiercest impact. **l)** Linear regression between the volume of BBB disruption (in %) and the integration of total strain rate (sum of the strain rate over all elements) in the fiercest impact (the impact in which the value maximizes). **m)** Linear regression between the average BBB disruption (expressed as slope) and the peak value of total strain rate in the fiercest impact. **n)** Linear regression between the average BBB disruption (expressed as slope) and the integration of strain rate in the fiercest impact. **o)** Linear regression between the volume of BBB disruption (in %) and the integration of total absorbed power (sum of the absorbed power over all elements) in the fiercest impact (the impact in which the value maximizes). **p)** Linear regression between the average BBB disruption (expressed as slope) and the peak value of total absorbed power in the fiercest impact. **q)** Linear regression between the average BBB disruption (expressed as slope) and the integration of absorbed power in the fiercest impact.

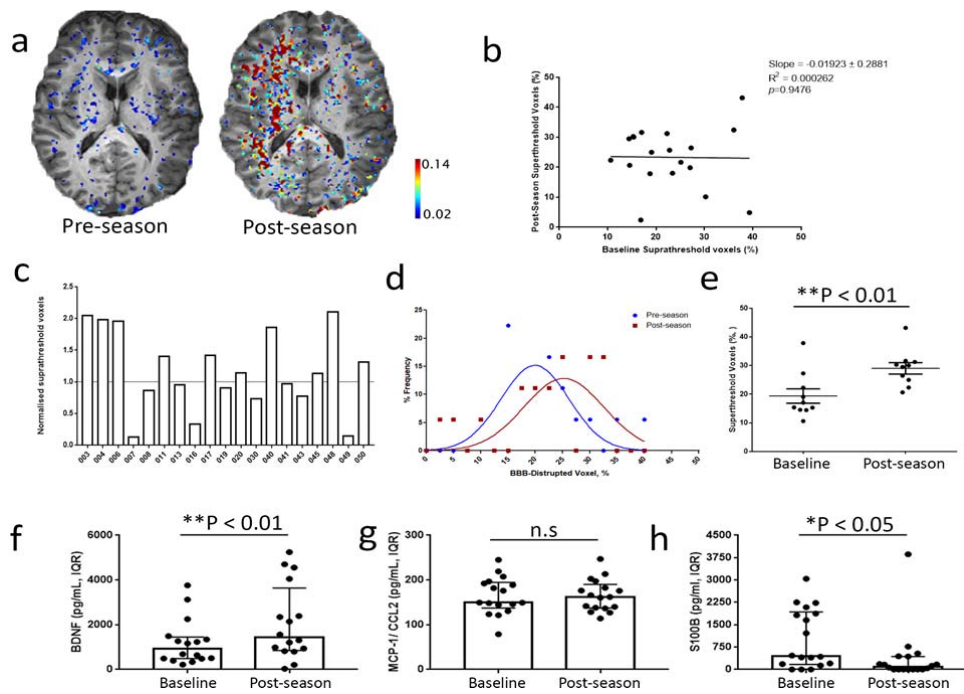


**Figure 2:** **a)** Enhanced gadolinium contrast agent (red) observed post-season in a youth rugby player (linear method). **b)** Linear regression between BBB disruption volume (in % voxels) at baseline vs post-season ( $n = 19$ ). **c)** Relative to baseline changes in volume of BBB disruption post-season ( $n = 19$ ). **d)** Distribution frequency of volume of BBB disruption (in % voxels) in players pre-season and post-season to ( $n = 19$ ). **e)** Increased BBB disruption volume (in % voxels) in players post-season compared to matched pre-season (\*\* $P < 0.001$ ), ( $n = 9$ ). **f)** Brain derived neurotrophic factor (BDNF) levels are significantly increased in players plasma post-season compared to pre-season (\*\* $P = 0.004$ ), ( $n = 16$ ). **g)** Monocyte chemoattractant protein-1 (MCP-1) levels are significantly increased in players plasma post-season compared to pre-season (\* $P = 0.01$ ), ( $n = 17$ ). **h)** Decreased levels of S100B detectable post-season compared to pre-season ( $P < 0.05$ ), ( $n = 17$ ).

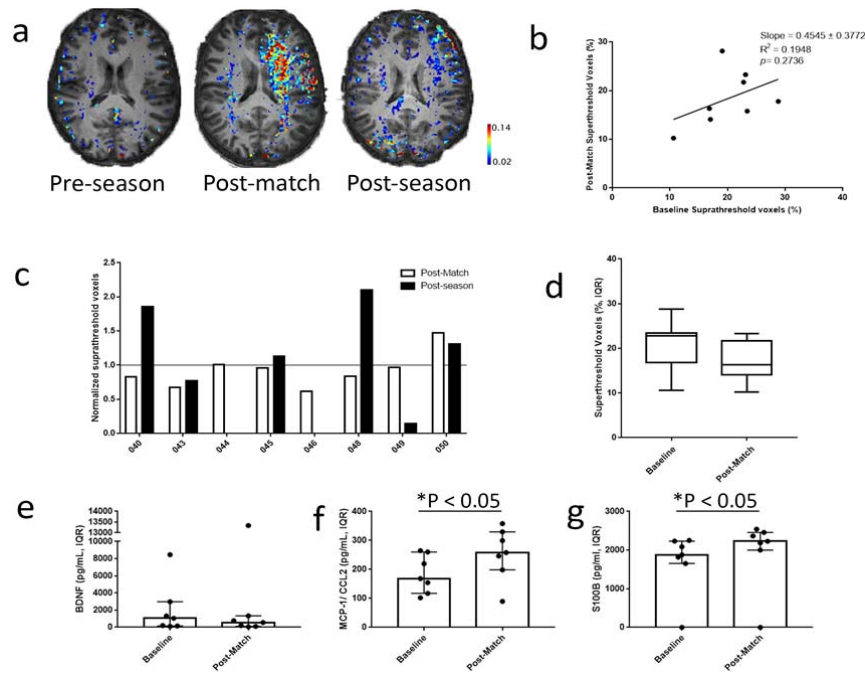


**Figure 3:** **a)** Enhanced gadolinium contrast agent (red) observed post-match and post-season in a university level rugby player (linear method). **b)** Linear regression between BBB disruption volume (in % voxels) at baseline vs post-match ( $n = 8$ ). **c)** Relative to baseline changes in volume of BBB disruption post-match and post-season ( $n = 8$ ). **d)** Non-significant changes in BBB disruption volume (in % voxels) post-match compared to baseline. **e)** Brain derived neurotrophic factor (BDNF) levels pre-season compared to post-match ( $n = 7$ ). **f)** Increased levels of monocyte chemoattractant protein-1 (MCP-1) post-match compared to pre-season ( $*P = 0.012$ ), ( $n = 7$ ). **g)** Increased levels of S100B observed post-match compared to pre-season ( $*P = 0.01$ ), ( $n = 7$ ).

## Pre-season/post season analysis

Variable	% voxels	S100 $\beta$	BDNF	MCP-1	
% voxels					$\pm 0.0-0.39$ No association
S100 $\beta$	-0.417				$\pm 0.4-0.59$ Weak association
BDNF	-0.057	0.320			$\pm 0.6-0.79$ Moderate association
MCP-1	-0.213	0.249	0.356		$\pm 0.8-1.0$ Strong association

## Pre-season/post match analysis

Variable	% voxels	S100 $\beta$	BDNF	MCP-1
% voxels				
S100 $\beta$	0.096			
BDNF	0.833	0.224		
MCP-1	0.410	0.332	0.175	

**Supplementary Figure 1:** Spearman's r-values correlating post-season suprathreshold voxel values with relative changes in serological markers of TBI and immune response markers in plasma samples. Relative changes were generated by normalising post-season concentrations to baseline values. **BDNF:** brain-derived neurotrophic factor. **MCP-1:** monocyte chemoattractant protein-1.

Supplementary Figure 2

Rugby cohort										
Concussion History				MRI Inclusion			MRI Dates			
Subject	Age	# Prior of Concussions	Most Recent Concussion	Time until resolution of symptoms	Hospitalisation	Baseline	Post-match	Post-Season	Post-Season time	Medication at assesment
School team										
1	17	1	> 6 months	≤1 hour	No	✓		✓	2 weeks	-
2	18	0	N.A.	-	No	✓		✓	3 weeks	Ibuprofin
3	17	1	> 3 months	≤24 hours	No	✓		✓	3 weeks	-
4	17	0	N.A.	-	No	✓		✓	3 weeks	-
5	17	0	N.A.	-	No	✓		✓	2 months	Ventolin
6	17	0	N.A.	-	No	✓		✓	2 months	-
7	16	1	> 2 yrs.	1 week	No	✓		✓	2 weeks	-
8	18	0	N.A.	-	No	✓		✓	3 weeks	-
9	17	0	N.A.	-	No	✓		✓	3 weeks	-
10	19	0	N.A.	-	No	✓		✓	1 week	-
11	18	0	N.A.	-	No	✓		✓	1 week	-
University team										
12	21	1	>6 months	5 days	No	✓	✓	✓	2 months	-
13	22	0	N.A.	-	No	✓	✓	✓	2 months	-
14	21	6	> 1 yr.	7 weeks	No	✓	✓	✓	2 months	Ventolin
15	23	1	> 2 yrs.	≤1 day	No	✓	✓	✓	2 months	-
16	21	2	> 1 yr.	1 week	No	✓	✓	✓	2 months	-
17	22	0	N.A.	-	No	✓	✓	✓	2 months	-
18	23	0	N.A.	-	No	✓	✓	✓	2 months	-
19	24	3	> 2 yrs.	6 days	No	✓	✓	✓	2 months	-
MMA cohort										
Concussion History				MRI Inclusion			MRI Dates			
Subject	Age	# Prior of Concussions	Most Recent Concussion	Time until resolution of symptoms	Hospitalisation	Baseline	Post-fight 1	Post-fight 2	Medication at assesment	
1	25	4	> 3 months	5 days	No	✓	✓		-	
2	26	0	N.A.	-	No	✓	✓		-	
3	28	1	> 1 yr.	≤24 hours	No	✓	✓		-	
4	24	1	> 2 yrs.	≤24 hours	No	✓	✓		-	
5	29	3	> 1 yr.	≤1 hour	No	✓	✓	✓	-	

Supplementary Figure 2: Demographics of rugby players and MMA fighters.